Characteristics of the anion transport system in sea turtle erythrocytes

ERICH K. STABENAU, CARLOS G. VANOYE, AND THOMAS A. HEMING
Pulmonary Research Laboratories, University of Texas Medical Branch, and National Marine Fisheries Service, Galveston, Texas 77550

STABENAU, ERICH K., CARLOS G. VANOYE, AND THOMAS A. HEMING. *Characteristics of the anion transport system in sea turtle erythrocytes* Am. J. Physiol. 261 (Regulatory Integrative Comp. Physiol. 30): R1218–R1225, 1991.—Erythrocytes of Kemp's ridley sea turtle (*Lepidochelys kempi*) contain a 100- to 105-kDa protein that is reactive with a monoclonal antibody to the membrane domain of human erythrocyte band 3. Based on inhibition of membrane HCO_3^--Cl^- exchange with 4-acetamido-4′-isothiocyanostilbene-2,2′-disulfonic acid (SITS), sea turtle erythrocytes were found to contain 4×10^6 copies of band 3 per cell. Unidirectional HCO_3^- transfer, specifically $HCO^-_{3\,out\rightarrow in}$-$Cl^-_{in\rightarrow out}$ exchange, where subscript in→out represents transfer from inside to outside and subscript out→in represents transfer from outside to inside, was characterized by a maximal exchange rate of 1.0–1.1 $nmol \cdot cm^{-2} \cdot s^{-1}$, substrate affinity coefficients of 0.1–0.2 mM for HCO_3^- and 1.6 mM for Cl^-, and an apparent inhibition constant for SITS of 0.6–1.0 μM (10°C, pH 7.6). Under physiological conditions (30°C, pH 7.4), the rate of net HCO_3^- transfer (i.e., the difference between $HCO^-_{3\,in\rightarrow out}$-$Cl^-_{out\rightarrow in}$ and $HCO^-_{3\,out\rightarrow in}$-$Cl^-_{in\rightarrow out}$) was 1.13 $nmol \cdot cm^{-2} \cdot s^{-1}$ for cells subjected to a 5-mM decrement in CO_2 content. This yields a rate coefficient for the "physiological" anion shift in sea turtle blood of 1.7 s^{-1}, indicating that the anion shift may require 2.6 s to reach 99% completion in vivo. The erythrocyte anion shift appears to be a potential rate-limiting step for capillary CO_2 exchange in these turtles.

band 3; anion exchange; erythrocyte; *Lepidochelys*; reptile

TRANSMEMBRANE HCO_3^- flux plays an important role in CO_2 transport and exchange and in regulation of intracellular and extracellular pH. In erythrocytes, membrane transport of HCO_3^- occurs primarily via Na-independent HCO_3^--Cl^- exchange involving band 3 protein. This exchange has been well described in human erythrocytes (15, 19, 33). Less information is available about HCO_3^--Cl^- exchange in the erythrocytes of other species. Erythrocyte HCO_3^--Cl^- exchange might be expected to vary between species because of species differences in the amount of band 3 protein in erythrocytes. For example, agnathan (*Entosphenus japonicus*, *Eptatretus stouti*) erythrocytes appear to have little or no band 3 protein (8, 24), whereas human erythrocytes have 7,000 copies/μm^2 of cell surface (19), llama (*Lama glama*) erythrocytes have 23,000 copies/μm^2 (18), and trout (*Salmo irideus*) erythrocytes may have 30,000 copies/μm^2 (25).

Sea turtles are among the largest and most active of extant reptiles. Their corresponding requirements for exchange of metabolic gases (O_2, CO_2) are high relative to those of most other reptiles. For this reason, sea turtles might be expected to possess efficient mechanisms for gas exchange, including erythrocyte HCO_3^--Cl^- exchange. No data are available in the literature regarding the kinetics of HCO_3^--Cl^- exchange in reptile erythrocytes. Moreover, although band 3 protein has been found in erythrocytes of a freshwater turtle (*Pseudemys scripta*) (7), its presence in erythrocytes of other reptiles is unknown.

In the present study, the anion transport system in erythrocytes of Kemp's ridley sea turtles (*Lepidochelys kempi*) was characterized using electrophoretic, immunological, and kinetic techniques. Kinetic studies were conducted to determine the rates of both unidirectional (θ_{uni}) and net (θ_{net}) HCO_3^- transfer across the erythrocyte membrane. The physiological function of erythrocyte anion exchange is net HCO_3^- transfer (i.e., the difference between $HCO^-_{3\,out\rightarrow in}$-$Cl^-_{in\rightarrow out}$ and $HCO^-_{3\,in\rightarrow out}$-$Cl^-_{out\rightarrow in}$, where subscript in→out represents transfer from inside to outside and subscript out→in represents transfer from outside to inside) in the presence of significant transmembrane gradients for HCO_3^-. The time course of this "physiological" anion shift is protracted when compared with the time course of anion exchange under steady-state conditions (i.e., in the absence of transmembrane anion gradients) because of the production/consumption of intracellular HCO_3^- that continues as long as the anion shift is incomplete (33). The rate coefficient of the anion shift in sea turtles was calculated and compared with information about the anion shift in other vertebrate species.

METHODS

Blood samples. Sea turtles utilized in the present study were captive-reared at the National Marine Fisheries Service, Galveston Laboratory, Galveston, TX. Blood was collected into heparinized syringes from the cervical sinus of unanesthetized animals (1–2 yr of age), as described previously (26). The blood samples were held overnight at 4°C before use in experiments.

Determination of θ_{uni}. θ_{uni} was measured using the method of Lambert and Lowe (22) with minor modifications. In this technique, the time course of extracellular pH (pH_o) is followed when a HCO_3^--free Cl^--rich erythrocyte pellet is mixed with a HCO_3^--rich Cl^--free medium of similar pH_o (see below for media composition). In the

presence of extracellular carbonic anhydrase (CA) activity, transmembrane HCO_3^--Cl^- exchange is rate limiting for the consequent change in pH_o, as Cl^- and HCO_3^- reequilibrate across the erythrocyte membrane. The initial rate of change in pH_o (dpH_o/dt) reflects the initial rate of anion exchange. Anion exchange under these conditions is unidirectional in the sense that, theoretically, Cl^- is the only exchangeable intracellular anion, and HCO_3^- is the only exchangeable extracellular anion. Consequently, the expected operational mode of the exchanger is solely $HCO_{3\,out\rightarrow in}^-$-$Cl_{in\rightarrow out}^-$.

θ_{uni} experiments were conducted as follows. Erythrocytes were isolated by centrifugation and were washed three to four times in 4–5 vol of an isotonic solution containing (in mM; pH 7.6) 155 NaCl, 6 KCl, 5 D-glucose, 1.5 $CaCl_2$, and 1 *N*-2-hydroxyethylpiperazine-*N'*-2-ethanesulfonic acid (HEPES; nominally CO_2-HCO_3^- free). The final cell pellet contained 5% trapped extracellular solution and was thermostated at 10°C. θ_{uni} was monitored by continuously measuring pH_o when 250 μl of the cell pellet were injected into 15 ml of test medium (see below) in a stirred thermostated (10°C) pH system (pH meter model PHM84, Radiometer). The test medium contained (in mM; pH 7.6) 320 sucrose, 5 HEPES, 1.5 Ca-gluconate or $CaCl_2$, 0–2 $NaHCO_3$, 0.005 bovine CA (380–520 Wilbur-Anderson U/ml), and 0–0.1 SITS. Note that the cells were not pre-incubated with SITS in an attempt to examine SITS inhibition of θ_{uni} under predominately reversible conditions. All chemicals were from Sigma Chemical (St. Louis, MO).

The initial dpH_o/dt was determined from the initial linear portion of the pH_o time course (≤2 s after pellet injection into the test medium). The response half-time of the electrode system in these studies was 850 ms, as measured for a step change from pH 4 to 8. Measurements of dpH_o/dt were corrected for the system half-time, assuming the observed reaction was first order (i.e., the observed reaction half-time equaled the sum of the true reaction half-time and the measurement system half-time).

Determination of θ_{net}. θ_{net} was measured using a stopped-flow method (12). In this technique, the time course of pH_o is followed when a HCO_3^--rich erythrocyte suspension was mixed with an acidic buffer (both media containing Cl^-, see below for compositions) in a stopped-flow apparatus. In the presence of extracellular CA activity, HCO_3^--Cl^- exchange is rate limiting for transmembrane H^+ equilibration, and the dpH_o/dt immediately after flow stops reflects the initial rate of anion exchange. Four operational modes of the exchanger are possible under these conditions (i.e., Cl^--Cl^-, HCO_3^--HCO_3^-, $HCO_{3\,in\rightarrow out}^-$-$Cl_{out\rightarrow in}^-$, and $HCO_{3\,out\rightarrow in}^-$-$Cl_{in\rightarrow out}^-$). The monitored reaction represents a net HCO_3^- transfer, specifically the difference between the rates of $HCO_{3\,in\rightarrow out}^-$-$Cl_{out\rightarrow in}^-$ exchange and $HCO_{3\,out\rightarrow in}^-$-$Cl_{in\rightarrow out}^-$ exchange.

Red blood cells for θ_{net} experiments were prepared as follows. Erythrocytes were isolated by centrifugation, washed three to four times in 4–5 vol of an isotonic solution [(in mM) 155 NaCl, 6 KCl, 5 D-glucose, 1.5 $CaCl_2$, and 1 HEPES; pH 7.6], and finally suspended at 10% hematocrit in the same solution. $NaHCO_3$ and bovine CA were added to yield concentrations of 10 mM and 800 Wilbur-Anderson U/ml, respectively. The cell suspension was titrated under strict anaerobic conditions to an equilibrium pH_o of 7.4 at 30°C (pH of cervical sinus blood at the measured turtle cloacal temperature) or to pH_o 7.6 at 10°C. SITS (0–100 μM) was added to aliquots of the suspension, and the aliquots were incubated for at least 30 min at the appropriate experimental temperature before studies were conducted. Consequently, studies of SITS inhibition of θ_{net} were conducted under predominately irreversible conditions (13).

θ_{net} was monitored by continuously measuring pH_o when equal volumes of a red blood cell suspension and an acidic buffer [(in mM) 157.5 NaCl, 6 KCl, 1.5 $CaCl_2$, and 11 HEPES; pH 6.7] were mixed in a thermostated (10 or 30°C) stopped-flow apparatus. This apparatus has been described in detail previously (12). The initial dpH_o/dt was determined from the first 500 ms (after flow stopped) of the pH_o time course. The response time of the electrode system in these studies, estimated using a ramp change in pH, was <5 ms and was ignored in subsequent data analyses.

Computations of HCO_3^- *transfer.* The initial transfer rate of acid-base equivalents across the red blood cell membrane per unit of cell surface area (θH^+) was calculated as

$$\theta H^+ = \frac{(dpH_o/dt)\beta_o(1 - Hct)}{Hct(A/V)} \qquad (1)$$

where β_o is the extracellular non-HCO_3^- buffer capacity at the initial pH_o (medium pH before pellet injection in θ_{uni} studies and pH_o under constant flow conditions in θ_{net} studies), Hct is mixture hematocrit, V is cell volume (391 μm^3), and A is cell surface area (457 μm^2). V and A were calculated from direct measurements of air-dried erythrocyte diameters (18.00 × 10.75 μm) using the equations of Westerman et al. (29) and assuming *1*) a 10% shrinkage of cells during air drying (9) and *2*) a cell thickness of 2.2 μm (34)

$$V = 0.712\ d^2T \qquad (2)$$

$$A = 2\pi a^2 + \frac{2\pi ab\ (\sinh^{-1}\epsilon)}{\epsilon} \qquad (3)$$

where d is equivalent cell diameter, T is cell thickness, a is $0.5d$, b is $0.67T$, and

$$\epsilon = \sqrt{a^2 - b^2}/a \qquad (4)$$

Neglecting OH^- flux under the conditions of our experiments, θH^+ equals the rate of HCO_3^--Cl^- exchange (θ_{uni}, θ_{net}).

As appropriate, θ_{uni} data were numerically fit to the Michaelis equation for an enzyme-catalyzed reaction

$$\theta_{uni} = ([HCO_3^-]_o V_{max})/(K_{1/2} + [HCO_3^-]_o) \qquad (5)$$

and to the Michaelis equation for noncompetitive inhibition

$$\theta_{uni} = \frac{[HCO_3^-]_o V_{max}}{K_{1/2}(1 + [SITS]/K_i) + [HCO_3^-]_o(1 + [SITS]/K_i)} \qquad (6)$$

and were analyzed using Hanes-Woolf ($[HCO_3^-]_o/\theta_{uni}$ vs. $[HCO_3^-]_o$) plots, where $[HCO_3^-]_o$ is extracellular HCO_3^-

concentration, V_{max} is maximal exchange rate, and [SITS] is SITS concentration. In addition, an Easson-Steadman plot of $1/(1 - I)$ vs. [SITS]/I (13, 28) was used to investigate SITS inhibition of θ_{uni}. In this analysis, I is the fractional inhibition of θ_{uni}, as determined from

$$I = 1 - \left(\frac{k_i}{k_c}\right) \quad (7)$$

where k_i is the rate coefficient for HCO_3^--Cl^- exchange in the presence of SITS, and k_c is the rate coefficient for control cells. Rate coefficients were calculated as

$$k = \frac{\theta_{uni} A}{[HCO_3^-]_o} \quad (8)$$

Biochemical characterization. Polyacrylamide gel electrophoresis (PAGE) in sodium dodecyl sulfate (SDS) was carried out according to Laemmli (21) and Jennings et al. (16) using gels with linear gradients of 4–10% polyacrylamide. Erythrocytes for electrophoretic studies were centrifuged, resuspended to 90% hematocrit, and hemolyzed in 9 vol of 5 mM $MgCl_2$. The lysate was diluted with 9 vol of Laemmli (21) buffer and heated at 100°C for 2 min. The final solution and prestained protein standards (Bethesda Research Laboratories, Gaithersburg, MD) were run on SDS-PAGE in duplicate. Proteins in one of the duplicate gels were stained with Coomassie Brilliant Blue. Proteins in the second gel were transferred electrophoretically to a polyvinylidene difluoride membrane (Immobilon-P membrane, Millipore, Bedford, MA) for protein (Western blot) analysis. Immunoblots were performed according to Towbin et al. (27) and Jennings et al. (17) using a monoclonal antibody against the membrane domain of human erythrocyte band 3 protein (mAb IV F 12). Incubations with primary antibody (mAb IV F 12 at 1:2,000 dilution) and secondary antibody (alkaline phosphatase-conjugated goat anti-mouse immunoglobulin G) were at 25°C for 12 and 3 h, respectively. The primary antibody was a kind gift from Dr. M. L. Jennings (University of Texas Medical Branch, Galveston, TX).

RESULTS

Electrophoretic and immunological characteristics. A SDS-PAGE of the erythrocyte proteins of Kemp's ridley sea turtle is shown in Fig. 1 together with the corresponding immunoblot. Sea turtle erythrocytes contained a 100- to 105-kDa protein that was reactive with the monoclonal antibody to the membrane domain of human erythrocyte band 3. Additional bands on the immunoblot reflected a cross-reactivity of the secondary antibody with erythrocyte protein(s) of ≤24 kDa.

Unidirectional HCO_3^- transfer. A rapid near-exponential decrease in mixture pH_o was observed when a nominally HCO_3^--free Cl^--rich pellet of turtle erythrocytes was mixed with a HCO_3^--rich Cl^--free medium of similar pH_o (Fig. 2*A*). The initial dpH_o/dt of this acidification was used to calculate θ_{uni} (see above). Changes in mixture pH_o (≤2 s after mixing) were abolished by inhibition of band 3-mediated anion exchange with 100 μM SITS (Fig. 2*A*), by inhibition of test medium CA with 100 μM acetazolamide, and by nominal omission of HCO_3^- from the test medium.

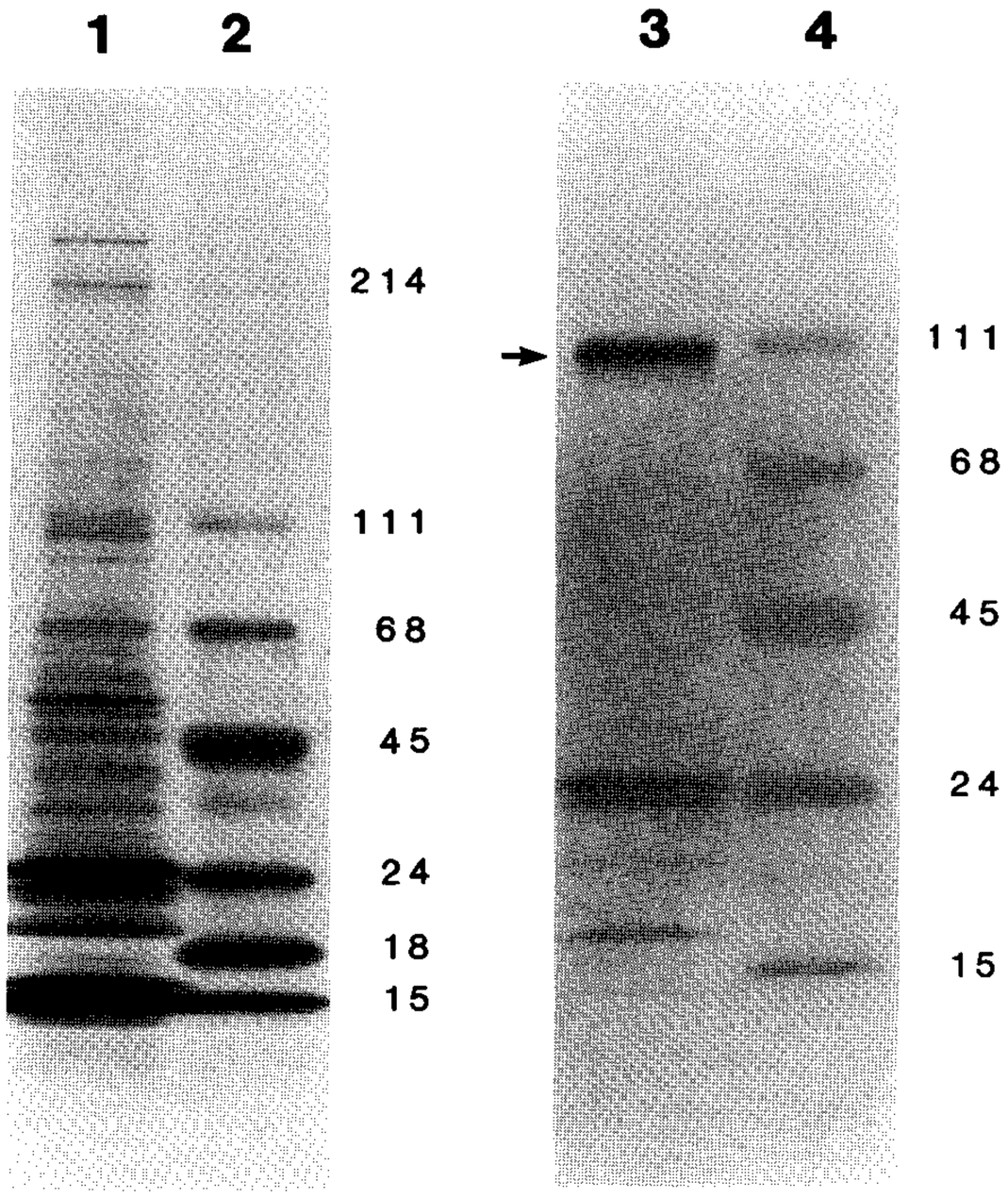

FIG. 1. Sodium dedecyl sulfate-polyacrylaminde gel electrophoresis of sea turtle erythrocyte proteins. *Lane 1*: sea turtle erythrocyte proteins stained with Coomassie Brilliant Blue. *Lane 2*: molecular mass standards [(in kDa) 214 myosin, 111 phosphorylase *b*, 68 bovine serum albumin, 45 ovalbumin, 24 α-chymotrypsinogen, 18 β-lactoglobulin, and 15 lysozyme] stained with Coomassie Brilliant Blue. *Lane 3*: immunoblot of sea turtle erythrocyte proteins using monoclonal antibody against membrane domain of human erythrocyte band 3 protein (mAb IV F 12). Arrow indicates band 3 protein. Other bands reflect cross-reactivity with secondary antibody. *Lane 4*: molecular mass standards as in *lane 2*.

θ_{uni} was dependent on $[HCO_3^-]_o$ and exhibited saturation kinetics with increasing $[HCO_3^-]_o$, consistent with a carrier-mediated process (Fig. 3*A*). The relationship between θ_{uni} and $[HCO_3^-]_o$ in the nominal absence of extracellular Cl^- was adequately described by the Michaelis equation ($\chi^2 = 0.082$, $P < 0.05$). This analysis yielded a substrate affinity coefficient ($K_{½}$) for HCO_3^- of 0.1 mM and a V_{max} of 1.0 nmol·cm^{-2}·s^{-1}.

SITS inhibited θ_{uni} in a dose-dependent manner (Fig. 3*B*). The median inhibitory concentration (IC_{50}) was 0.6–1.1 μM. Figure 4*A* gives Hanes-Woolf plots of θ_{uni} at each [SITS] vs. $[HCO_3^-]_o$. The plots intersect on the *x*-axis, suggesting noncompetitive inhibition. The slopes of these plots equal $1/V_{max\ app}$ (where $V_{max\ app}$ is the apparent V_{max} in the presence of SITS), and the *x*-intercepts equal the negative $K_{½}$. These analyses yielded a $K_{½}$ for HCO_3^- of 0.1–0.2 mM and a V_{max} (at 0 μM SITS) of 1.1 nmol·cm^{-2}·s^{-1}. A plot of $1/V_{max\ app}$ vs. [SITS] (plot not shown) yielded a K_i for SITS (negative *x*-intercept) of 0.7 μM. On the basis of these results, the data for θ_{uni} at each $[HCO_3^-]_o$ vs. [SITS] (Fig. 3*B*) were numerically fit to the Michaelis equation for noncompetitive inhibition ($\chi^2 = 0.019$–0.063, $P < 0.05$). These analyses provided still additional estimates of the $K_{½}$ for HCO_3^- of 0.1 mM, V_{max}

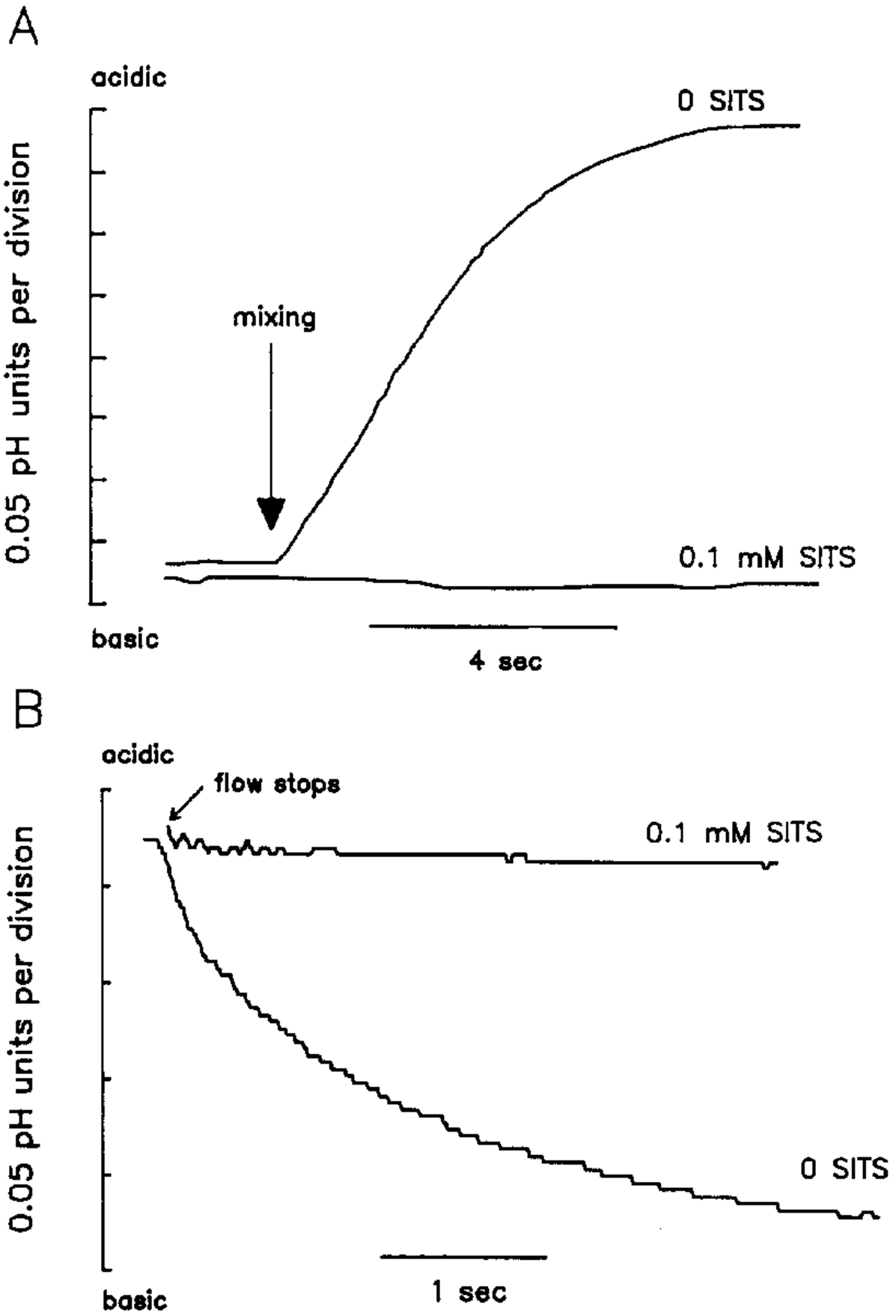

FIG. 2. Representative traces of extracellular pH (pH_o) in presence and absence of 100 μM SITS. *A*: pH_o time course after mixing Cl^--rich nominally HCO_3^--free pellet of erythrocytes with Cl^--free HCO_3^--rich medium at 10°C. Changes in pH_o reflect re-equilibration of HCO_3^- across erythrocyte membrane. Initial rate of change in pH_o (dpH_o/dt) was used to calculate rate of unidirectional transfer across erythrocyte membrane (θ_{uni}). *B*: pH_o time course after mixing HCO_3^--rich suspension of erythrocytes (pH 7.4) with acidic buffer solution (pH 6.7) in stopped-flow apparatus at 30°C. Changes in pH_o after flow stopped reflect re-equilibration of H^+ across erythrocyte membrane via Jacobs-Stewart cycle. dpH_o/dt immediately after flow stopped was used to calculate rate of net transfer across erythrocyte membrane (θ_{net}).

of 1.0 nmol·cm^{-2}·s^{-1}, and K_i for SITS of 0.6–1.0 μM.

At each $[HCO_3^-]_o$, θ_{uni} was significantly reduced by 3 mM of extracellular Cl^- (Fig. 3*A*). Hanes-Woolf plots of θ_{uni} at each extracellular Cl^- concentration ($[Cl^-]_o$) vs. $[HCO_3^-]_o$ are given in Fig. 4*B*. The plots intersect below the *x*-axis and to the left of the *y*-axis, indicating mixed competitive-noncompetitive inhibition. Assuming Cl^- behaved as a simple linear mixed-type inhibitor, we plotted $K_{m\,app}/V_{max\,app}$ (*y*-intercept of Hanes-Woolf plot, where $K_{m\,app}$ is the apparent Michaelis constant in the presence of Cl^-) vs. the nominal $[Cl^-]_o$ (plot not shown). The analysis yielded a K_i (negative *x*-intercept) or, more appropriately, a $K_{½}$ for Cl^- of 1.6 mM. It is worth noting that this value provides only an approximation of the true $K_{½}$ for Cl^- because of uncertainty about the actual $[Cl^-]_o$.

An Easson-Steadman plot for θ_{uni} is given in Fig. 5.

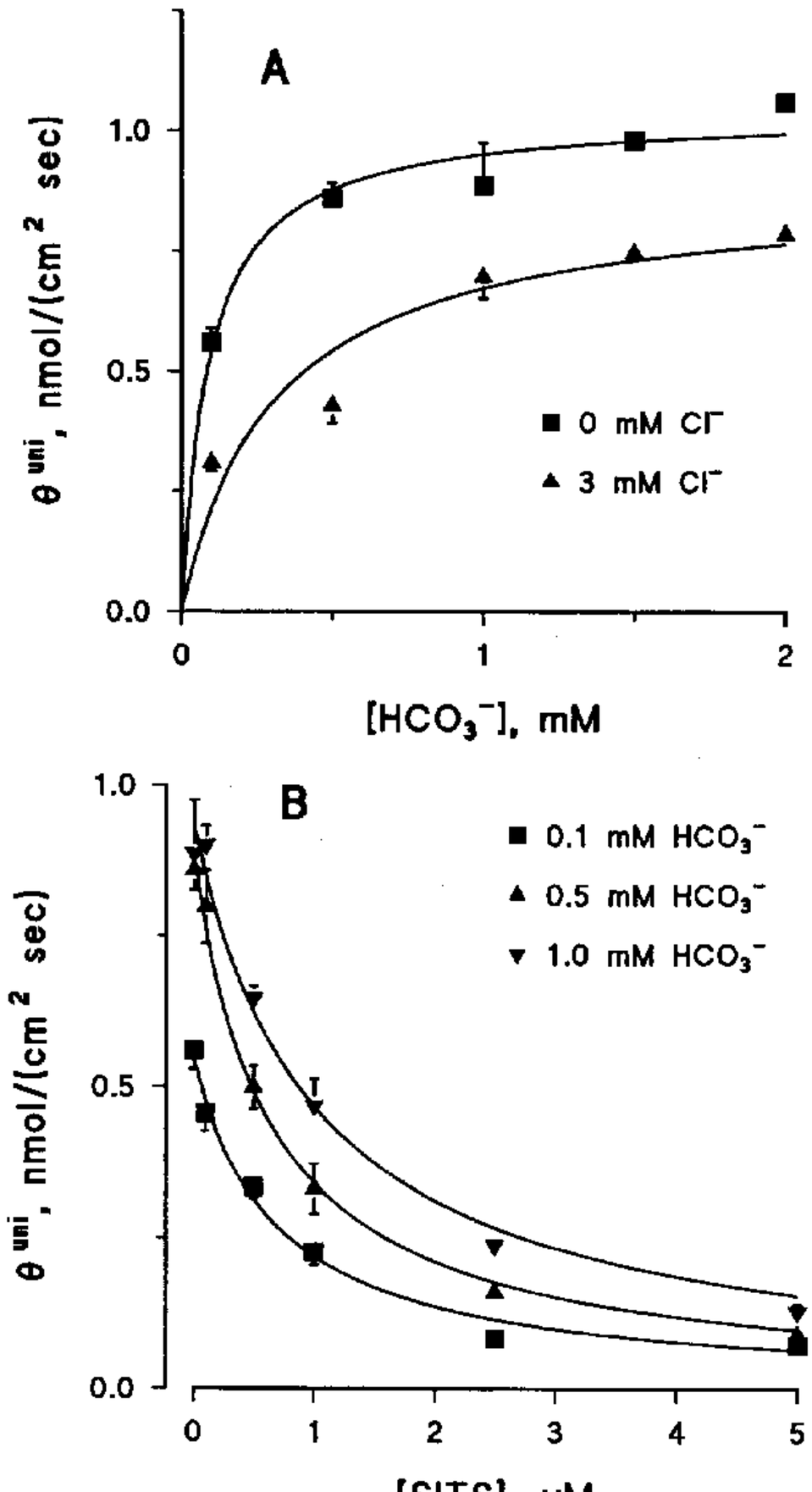

FIG. 3. Rate of unidirectional $HCO_{3\,out\rightarrow in}^-$-$Cl^-_{in\rightarrow out}$ exchange (θ_{uni}), where subscript in→out represents transfer from inside to outside and subscript out→in represents transfer from outside from inside, in sea turtle erythrocytes at 10°C (mean ± SE). *A*: effect of extracellular HCO_3^- concentration ($[HCO_3^-]_o$) in presence and absence of extracellular Cl^-. Lines are numerical fits of data to Michaelis equation (χ^2 = 0.082–0.213) and yield substrate affinity constant ($K_{½}$) for HCO_3^- (0 mM extracellular Cl^-) of 0.1 mM and maximal exchange rate (V_{max}) of 1.0 nmol·cm^{-2}·s^{-1}. *B*: effect of SITS at various $[HCO_3^-]_o$ (0 mM extracellular Cl^-). Lines are numerical fits of data to Michaelis equation for noncompetitive inhibition (χ^2 = 0.019–0.063) and yield $K_{½}$ for HCO_3^- of 0.1 mM, a V_{max} of 1.0 nmol·cm^{-2}·s^{-1}, and an inhibitory constant for SITS of 0.6–1.0 μM. [SITS], SITS concentration.

The reciprocal of the slope of this plot yielded a dissociation constant (K_d) for the "SITS binding site" reaction of 0.6 μM. The *y*-intercept (which equals the negative quotient of the total concentration of SITS binding sites and K_d) can be used to provide an indirect determination of the number of binding sites per unit of cell membrane surface area (see Ref. 13). In this way, sea turtle erythrocytes were calculated to contain 8,000 SITS binding sites/μm^2, presumably indicating an equal density of band 3 protein.

Net HCO_3^- transfer. Figure 2*B* gives a representative trace of the change in pH_o when a HCO_3^--rich suspension of turtle erythrocytes (30°C, pH_o 7.4) was mixed with an acidic buffer (pH_o 6.7) in a stopped-flow apparatus. After flow stopped, mixture pH_o increased rapidly as trans-

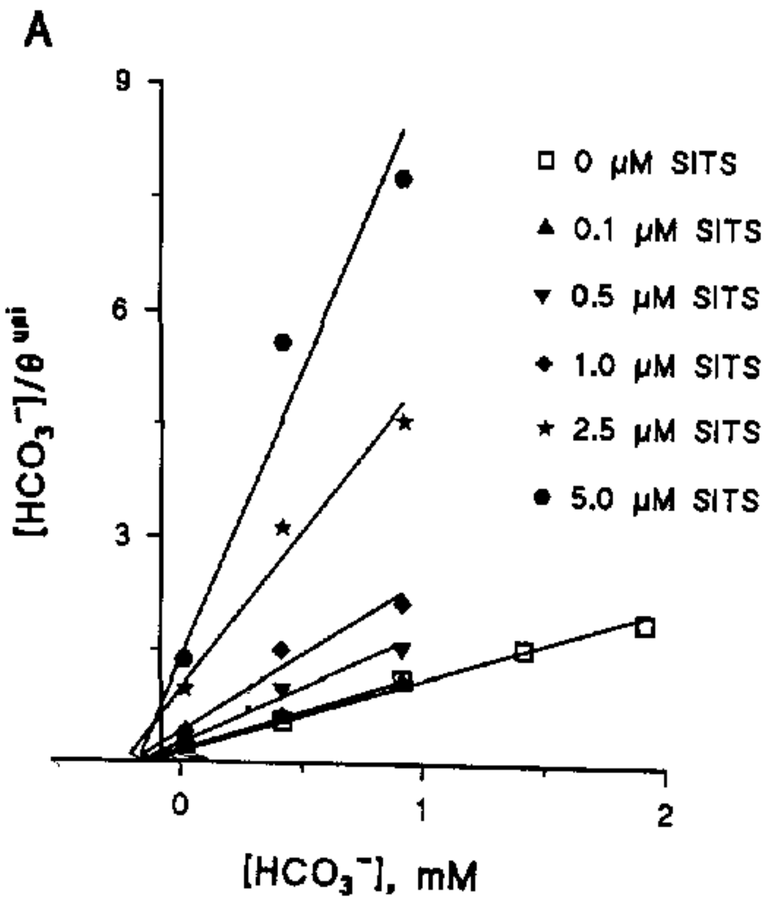

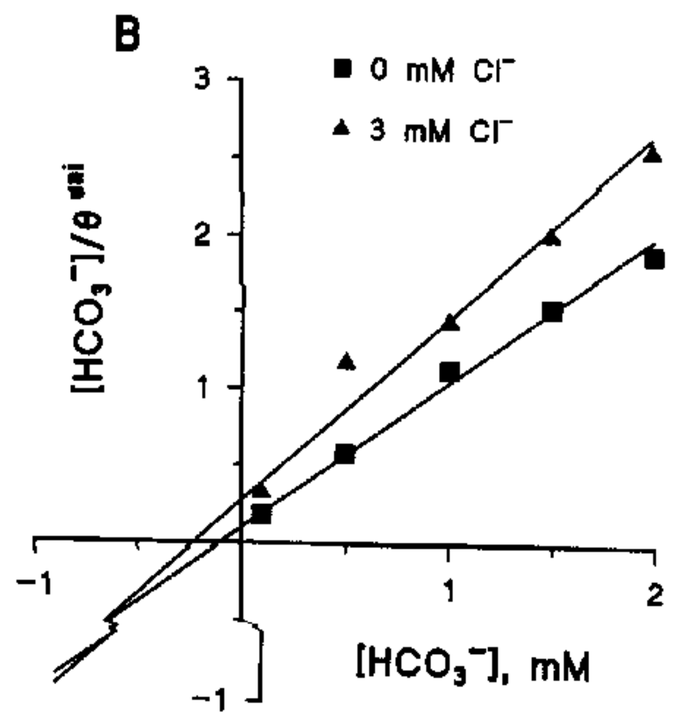

FIG. 4. Hanes-Woolf plots of θ_{uni} and $[HCO_3^-]_o$. *A*: effect of SITS (0 mM extracellular Cl^-). Lines are least-squares regression fits of data ($r = 0.969$–0.999) and yield $K_{1/2}$ for HCO_3^- of 0.1–0.2 mM and V_{max} (0 mM SITS) of 1.1 nmol·cm^{-2}·s^{-1}. *B*: effect of extracellular Cl^- (0 mM SITS). Lines are least-squares regression fits of data ($r = 0.984$–0.996).

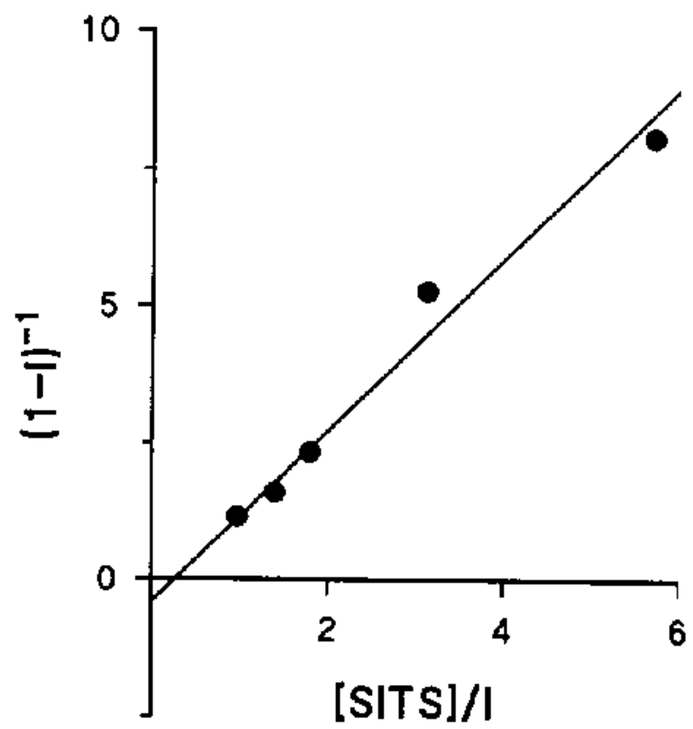

FIG. 5. Easson-Steadman plot of fractional inhibition of θ_{uni} (I) and SITS concentration ([SITS]). Line is least-squares regression fit of data ($r = 0.988$) and yields dissociation constant for SITS binding site reaction of 0.6 μM and density of SITS binding sites of 8,000/μm^2 of erythrocyte membrane.

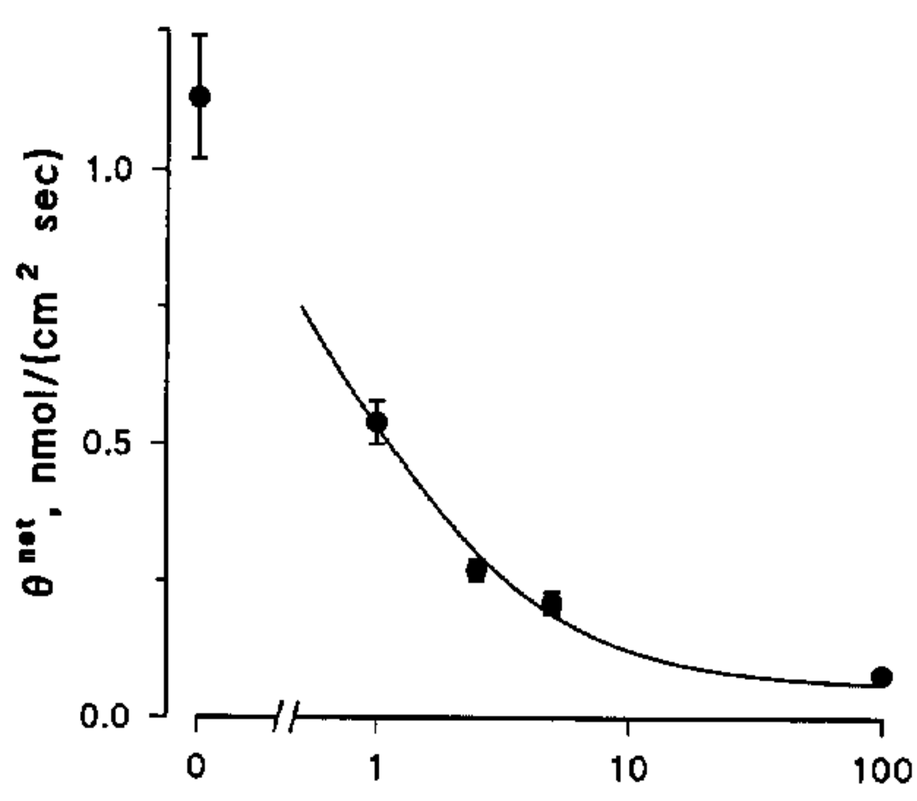

FIG. 6. Effect of SITS on rate of net HCO_3^- transfer (θ_{net}) in sea turtle erythrocytes at 30°C expressed as means ± SE. Line is numerical fit of data to sigmoid power curve and yields median inhibitory concentration of 0.8 μM.

membrane H^+ equilibration was reached via the Jacobs-Stewart cycle. The initial dpH_o/dt immediately after stopping flow was used to calculate θ_{net} (see above). The alkalinization reaction was abolished by inhibition of band 3-mediated anion exchange with 100 μM SITS (Fig. 2*B*).

θ_{net} averaged 0.43 ± 0.03 (SE) nmol·cm^{-2}·s^{-1} under conditions comparable to those of the unidirectional transfer studies (10°C, pH_o 7.6). When determined under physiological conditions (30°C, pH_o 7.4), θ_{net} averaged 1.13 ± 0.11 nmol·cm^{-2}·s^{-1}. SITS inhibited θ_{net} with an IC_{50} of 0.8 μM at 30°C (Fig. 6).

DISCUSSION

Erythrocytes of Kemp's ridley sea turtles contain a 100- to 105-kDa band 3 protein (Fig. 1). The apparent molecular weight of sea turtle erythrocyte band 3 is intermediate between that of mammalian erythrocytes (88–98 kDa; Refs. 18, 19, 33) and fish erythrocytes (116 kDa; Ref. 23). Sea turtle band 3 migrated on SDS gels as a single diffuse band like human erythrocyte band 3 (17) and unlike chicken erythrocyte band 3 protein, which migrates as 2 bands (14).

Easson-Steadman plots (Fig. 5) can be used to provide an indirect determination of the concentration of SITS binding sites (see Ref. 13). Assuming a one-to-one binding of SITS to band 3 (4), sea turtle erythrocytes appear to contain ~8,000 band 3 copies/μm^2 of cell surface. It should be pointed out that this calculation is highly dependent on erythrocyte surface area and volume, values that were also indirectly determined in the present study. The present data suggest that the density of band 3 in sea turtle erythrocytes is similar to that in human erythrocytes (7,000 copies/μm^2; Ref. 19). In contrast, the erythrocytes of llamas contain 23,000 copies/μm^2 (18), and trout contain 30,000 copies/μm^2 (25). When compared on a copies-per-cell basis to account for the vastly different sizes of the erythrocytes of these species, sea turtles are found to contain 4×10^6 copies/cell ($A = 457$ μm^2), trout to contain 8×10^6 copies/cell ($A = 260$ μm^2; Ref. 25), and humans and llamas to contain 1×10^6 copies/cell ($A = 142$ and 43 μm^2, respectively; Refs. 18, 19). Thus, there is no obvious correlation between the prevalence of band 3 protein (expressed either as copies/μm^2 or copies/cell) and erythrocyte size or shape (ellip-

tical disks in turtles, trout, and llamas vs. biconcave disks in humans).

The maximum rate of unidirectional anion exchange (V_{max} of θ_{uni}) determined using the technique of Lambert and Lowe (22) should theoretically approach the total anion transport capacity of erythrocytes (33). The total anion transport capacity of human erythrocytes is 40–50 $nmol \cdot cm^{-2} \cdot s^{-1}$ at 38°C and decreases to 1–2 $nmol \cdot cm^{-2} \cdot s^{-1}$ at 10°C (1, 2, 31–33). Thus, at the same temperature (10°C), the total transport capacity of sea turtle erythrocytes (1.0–1.1 $nmol \cdot cm^{-2} \cdot s^{-1}$) is similar to that of human erythrocytes. Given that sea turtle and human erythrocytes contain similar densities of band 3 protein (8,000 vs. 7,000 copies/μm^2, respectively), these data suggest that the anion transport systems in sea turtle and human erythrocytes have similar turnover numbers at 10°C. Sea turtle erythrocytes differ from trout erythrocytes in this regard. Romano and Passow (25) reported that trout and human erythrocytes have similar rates of equilibrium Cl^- exchange at 10–15°C, despite finding that the density of band 3 (copies/μm^2) in trout erythrocytes was 4.3 times that of human erythrocytes. This indicates that, at 10–15°C, the turnover number of the anion transport system of trout erythrocytes is substantially less than that of the human system.

The anion transport systems of sea turtle and human erythrocytes have similar substrate affinities. Comparable data are not available for the erythrocytes of other species. The $K_{½}$ values for HCO_3^- (0.1–0.2 mM) and Cl^- (1.6 mM) of sea turtle erythrocytes at 10°C are in general agreement with, albeit approximately one-half of, those determined by Lambert and Lowe (22) for human erythrocytes at the same temperature in the presence of similar transmembrane anion gradients ($K_{½}$ for HCO_3^- of 0.3–0.7 mM and $K_{½}$ for Cl^- of 4 mM). The anion transport system of human erythrocytes has a higher affinity for HCO_3^- than for Cl^- (19). Lambert and Lowe (22) reported a 10-fold difference between the $K_{½}$ for HCO_3^- vs. Cl^- of human erythrocytes. Our data indicate a similar difference exists between the $K_{½}$ for HCO_3^- vs. Cl^- (8- to 16-fold) in sea turtle erythrocytes. The $K_{½}$ values of human erythrocytes are temperature dependent, increasing with increments in temperature (1, 10). Consequently, the $K_{½}$ values obtained for sea turtle erythrocytes at 10°C probably underestimate the substrate affinity coefficients at physiological temperatures.

The $K_{½}$ values of sea turtle erythrocytes determined in the presence of transmembrane anion gradients are more than an order of magnitude lower than the substrate dissociation constants (K_s) reported for human erythrocytes under steady-state conditions (K_s for HCO_3^- of 16 mM and K_s for Cl^- of 65–67 mM; Ref. 19). Differences between determinations of $K_{½}$ obtained in the presence of transmembrane anion gradients and K_s obtained under steady-state conditions can be explained by asymmetry in the band 3 anion exchanger. The anion transport system of erythrocytes displays both extrinsic and intrinsic asymmetry (11, 15, 19). Extrinsic asymmetry is consistent with the Ping-Pong model of anion exchange, as a consequence of transmembrane Cl^- gradients. According to the Ping-Pong model, binding, transport, and dissociation of an anion in one direction obligatorily precedes binding, transport, and dissociation of an anion moving in the opposite direction. In the presence of a transmembrane Cl^- gradient, the number of inward-facing and outward-facing transport sites differ, with more sites facing the compartment with the lowest [Cl^-] (i.e., the intracellular compartment under physiological conditions). There is additional evidence that the anion transport system of erythrocytes displays intrinsic asymmetry; more transport sites appear to face the intracellular compartment, even in the absence of transmembrane Cl^- gradients (20).

In the present unidirectional transfer studies, the predicted intracellular [Cl^-] of sea turtle erythrocytes before cell injection into the test medium was 70–75 mM, given the measured Donnan H^+ ratio of 0.60. Thus, before sea turtle erythrocytes were injected into the test medium, the majority of anion transport sites presumably were facing inward. On mixing with the Cl^--free medium, the transmembrane Cl^- gradient was reversed, and chloride ions were translocated from inside to outside the cells. Bicarbonate ions then bound to the now outward-facing sites and were translocated inside the cell. The cycle repeated until HCO_3^- and Cl^- re-equilibrated across the cell membrane. It follows that, under the present experimental conditions, $K_{½}$ values primarily reflected inward-directed anion transfer and were determined primarily by the substrate affinity of the outward-facing site ($K_{m\,out}$) and the rate constant for anion translocation across the cell membrane from outside to inside ($k_{out \rightarrow in}$). In contrast, K_s determinations under steady-state conditions are a function of the binding affinity for substrate to both inward- and outward-facing sites ($K_{m\,in}$ and $K_{m\,out}$, respectively) and the rate constants for anion translocation across the cell membrane in both directions ($k_{in \rightarrow out}$ and $k_{out \rightarrow in}$). Previous investigators (11) have shown that the $K_{½}$ for inward-directed transfer is 15-fold less than the $K_{½}$ for outward-directed transfer. It is unclear whether this asymmetry arises from differences between $K_{m\,in}$ vs. $K_{m\,out}$, differences between $k_{in \rightarrow out}$ vs. $k_{out \rightarrow in}$, or a combination of the two (15).

HCO_3^--Cl^- exchange in sea turtle erythrocytes was inhibited by SITS in a dose-dependent manner (for θ_{uni}: IC_{50} of 0.6–1.1 μM, K_i of 0.6–1.0 μM, and K_d of 0.6 μM; for θ_{net}: IC_{50} of 0.8 μM). Cabantchik and Rothstein (4) reported a K_i of SITS for anion exchange in human erythrocytes of 10 μM. Sea turtle erythrocytes, therefore, appear to have a higher affinity for SITS than do human erythrocytes. SITS exhibited apparent noncompetitive behavior toward θ_{uni} under the present experimental conditions. Binding of stilbene disulfonates to human erythrocyte band 3 involves two distinct phases, an initial reversible phase followed by irreversible binding (13). It is generally held that, under reversible conditions, stilbenes are competitive inhibitors of anion exchange, at least in human erythrocytes (15, 19, 33). However, once irreversibly bound, stilbenes can be expected to exhibit apparent noncompetitive behavior. Although the rate constants for covalent binding of SITS are not known, Janas et al. (13) gives the rate coefficient for covalent binding of 4,4′-diisothiocyanostilbene-2,2′-disulfonic acid (DIDS) to human erythrocyte band 3 as 0.03 min^{-1} at 10°C (experimental temperature of present θ_{uni} stud-

ies), yielding a half-time for covalent DIDS binding of 23 min. Assuming similar behavior by SITS, one would expect very little irreversible binding of SITS to sea turtle band 3 during the ≤2-s period considered in our determinations of θ_{uni}. Nonetheless, there are two plausible interpretations of our SITS data. First, SITS may indeed be a noncompetitive inhibitor of the anion transport system in sea turtle erythrocytes. Differences between human and sea turtle cells in this regard could be a species effect. A second possibility is that the rate coefficient for covalent binding of stilbenes to sea turtle band 3 may be markedly less than that for covalent binding to human band 3. If this is the case, the observed kinetics of SITS inhibition could reflect irreversible binding to sea turtle band 3.

Extracellular chloride behaved as a mixed competitive-noncompetitive inhibitor of θ_{uni} in sea turtle erythrocytes. This suggests that the anion transport system of sea turtle erythrocytes contains an external modifier site capable of substrate inhibition, similar to that documented for the anion transport system of human erythrocytes (15, 19, 33).

Physiological implications. Erythrocyte anion transfer is a potential rate-limiting step for capillary CO_2 exchange. The time course of anion transfer under physiological conditions is longer than that of equilibrium anion exchange under steady-state conditions because of the production/consumption of intracellular HCO_3^- (33). As defined by Wieth and Brahm (33), the rate coefficient of the physiological anion shift (k_{sys}) is the quotient of the maximum net transport of HCO_3^- (equivalent to our θ_{net}) and the total amount of HCO_3^- exchanged across the cell per unit of cell surface area. Table 1 compares this information for sea turtle and human blood. There is considerable difference between the k_{sys} of sea turtle and human blood. This difference is due in part to the smaller erythrocyte surface area per unit of blood volume in sea turtles (i.e., product of hematocrit and membrane surface area/unit cell vol). Also, differences in body temperature probably influence k_{sys}, because the half-time of erythrocyte anion exchange increases with decrements in temperature (1, 6, 25, 33). From the k_{sys} values given in Table 1, one calculates that sea turtle blood requires 0.4 s for 50% completion of the physiological anion shift after a change in CO_2 content and 2.6 s for 99% completion. Similar data are not available for other poikilotherms. For trout erythrocytes, however, Romano and Passow (25) reported half-times for equilibrium Cl^- exchange of 0.8–1.3 s at 10–15°C. Such values must be regarded as minimum estimates of the half-time of the physiological anion shift for reasons outlined by Wieth and Brahm (33). The half-times for equilibrium Cl^- exchange in trout erythrocytes are two- to threefold larger than the present estimate of the half-time of the physiological anion shift in sea turtle blood. This suggests that the physiological anion shift in trout blood at 10–15°C may require >5–8 s to achieve 99% completion after a change in CO_2 content.

Capillary transit time ultimately determines whether capillary CO_2 exchange is rate limited by erythrocyte anion transfer. Erythrocyte anion transfer can be expected to rate limit capillary CO_2 exchange whenever the 99% completion time of the physiological anion shift exceeds the capillary transit time. For example, the anion shift in human blood reaches ≥99% completion during pulmonary capillary transit at rest (transit time 750 ms) but ≤90% completion during pulmonary capillary transit during exercise (transit time 300 ms) (33). In turtles, normal capillary transit times are difficult to assess because of the cyclic nature of their cardiac output and because of the extent of intracardiac shunting of blood in relation to lung ventilation. Turtles are intermittent breathers and possess a three-chambered heart. During lung ventilation, cardiac output increases rapidly (as much as 2-fold), and the majority of blood flow is directed to the lungs. Conversely, during apnea, cardiac output falls gradually, and the majority of blood flow is directed to the systemic circulation. Cardiac output also varies markedly as a function of body temperature. In *Pseudemys scripta*, for example, cardiac output increases from 8.5 $ml \cdot kg^{-1} \cdot min^{-1}$ at 10°C to 84.5 $ml \cdot kg^{-1} \cdot min^{-1}$ at 30°C (30). Capillary transit times in the pulmonary and systemic circuits are expected to vary in parallel with these changes in blood flow.

In addition to rate-limiting capillary CO_2 exchange, noncompletion of the erythrocyte anion shift during capillary transit will result in significant CO_2-HCO_3^--H^+ disequilibria in postcapillary blood (5). The presence of such disequilibria in vivo could explain differences observed between alveolar gas P_{CO_2} and left pulmonary

TABLE 1. *Rates of physiological anion shift after step changes in blood CO_2 content*

Temp, °C	Hct, %	Membrane SA, μm^2/l cells	ΔC_{CO_2}, nmol/l blood	M_{total}, nmol/cm^2	θ_{net}, nmol/cm^2 s	k_{sys}, s^{-1}	Completion Time, s		
							50%	90%	99%
				Human					
38	40	1,575	1.9	0.15	0.9	6	0.12	0.38	0.76
38	40	1,575	6	0.48	3.1	6.5	0.11	0.35	0.70
37	40	1,575	2.5	0.20	1.33	6.7	0.10	0.34	0.68
				Sea turtle					
30	30	1,169	5	0.68	1.13	1.7	0.41	1.3	2.6

Temp, temperature; Hct, hematocrit; SA, surface area; ΔC_{CO_2}, step change in blood CO_2 content; M_{total}, total amount of HCO_3^- exchanged/SA; θ_{net} rate of net HCO_3^- transfer; k_{sys}, rate coefficient of anion shift. All data for 38°C groups are from Wieth and Brahm (33). Data for 37°C are calculated from data of Crandall et al. (6) with Hct and SA given by Wieth and Brahm (33). Data for 30°C are calculated from present results with Hct given by Stabenau et al. (26).

venous P_{CO_2} in turtles. The equilibrated P_{CO_2} of blood leaving turtle lungs (Pa_{CO_2}) has been reported to exceed the alveolar P_{CO_2} (PA_{CO_2}) (3). This disparity is consistent with a postcapillary continuance of the erythrocyte anion shift. Persistence of the erythrocyte anion shift in the postcapillary vasculature is expected to cause a postcapillary rise in blood P_{CO_2} and pH (5). Under such circumstances, the gas tensions and pH values of equilibrated postcapillary blood samples (i.e., Pa_{CO_2}, Pa_{O_2}, and pH_a) do not reflect the true gas tensions and pH of end-capillary blood (i.e., Pc_{CO_2}, Pc_{O_2}, and pH_c), specifically $Pa_{CO_2} > Pc_{CO_2} \approx PA_{CO_2}$, and $pH_a > pH_c$. The possible existence of postcapillary CO_2-HCO_3^--H^+ disequilibria in sea turtle blood in vivo warrants further investigation.

Dr. L. Starke and R. Schultz provided technical assistance with the biochemical studies. Drs. A. Bidani and M. L. Jennings provided constructive criticisms of the manuscript.

These studies were conducted under United States Fish and Wildlife Service Endangered and Threatened Species Permit no. PRT-676379. Financial support was provided by National Oceanic and Atmospheric Administration Grant NA89AA-D-SG139 Sea Grant to T. A. Heming.

Address for reprint requests: T. A. Heming, Dept. of Internal Medicine, Pulmonary Division, Route H76, University of Texas Medical Branch, Galveston, Texas 77550.

Received 25 February 1991; accepted in final form 7 June 1991.

REFERENCES

1. BRAHM, J. Temperature-dependent changes of chloride transport kinetics in human red cells. *J. Gen. Physiol.* 70: 283–306, 1977.
2. BRAHM, J., AND P. D. WIMBERLEY. Chloride and bicarbonate transport in fetal red cells. *J. Physiol. Lond.* 419: 141–156, 1989.
3. BURGGREN, W. W., AND G. SHELTON. Gas exchange and transport during intermittent breathing in chelonian reptiles. *J. Exp. Biol.* 82: 75–92, 1979.
4. CABANTCHIK, Z. I., AND A. ROTHSTEIN. The nature of the membrane sites controlling anion permeability of human red blood cells as determined by studies with disulfonic stilbene derivatives. *J. Membr. Biol.* 10: 311–330, 1972.
5. CRANDALL, E. D., AND A. BIDANI. Effect of red blood cell HCO_3^-/Cl^- exchange kinetics on lung CO_2 transfer: theory. *J. Appl. Physiol.* 50: 265–271, 1981.
6. CRANDALL, E. D., A. L. OBAID, AND R. E. FORSTER. Bicarbonate-chloride exchange in erythrocyte suspensions: stopped-flow pH measurements. *Biophys. J.* 24: 35–47, 1978.
7. DRENCKHAHN, D., M. OELMANN, P. SCHAAF, M. WAGNER, AND S. WAGNER. Band 3 is the basolateral anion exchanger of dark epithelial cells of turtle urinary bladder. *Am. J. Physiol.* 252 (*Cell Physiol.* 21): C570–C574, 1987.
8. ELLORY, J. C., M. W. WOLOWYK, AND J. D. YOUNG. Hagfish (*Eptatretus stouti*) erythrocytes show minimal chloride transport activity. *J. Exp. Biol.* 129: 377–383, 1987.
9. FRAIR, W. Sea turtle red blood cell parameters correlated with carapace lengths. *Comp. Biochem. Physiol. A Comp. Physiol.* 56: 467–472, 1977.
10. GLIBOWICKA, M., B. WINCKLER, N. ARANÍBAR, M. SCHUSTER, H. HANSSUM, H. RÜTERJANS, AND H. PASSOW. Temperature dependence of anion transport in the human red blood cell. *Biochim. Biophys. Acta* 946: 345–358, 1988.
11. GUNN, R. B., AND O. FRÖHLICH. Asymmetry in the mechanisms for anion exchange in human red blood cell membranes. Evidence for reciprocating sites that react with one transported anion at a time. *J. Gen. Physiol.* 74: 351–374, 1979.
12. HEMING, T. A., C. G. VANOYE, AND A. BIDANI. Dipyridamole inhibition of HCO_3^--Cl^- exchange in human erythrocytes. *J. Pharmacol. Exp. Ther.* 255: 631–635, 1990.
13. JANAS, T., P. J. BJERRUM, J. BRAHM, AND J. O. WIETH. Kinetics of reversible DIDS inhibition of chloride self exchange in human erythrocytes. *Am. J. Physiol.* 257 (*Cell Physiol.* 26): C601–C606, 1989.
14. JAY, D. G. Characterization of the chicken erythrocyte anion exchange protein. *J. Biol. Chem.* 258: 9431–9436, 1983.
15. JENNINGS, M. L. Structure and function of the red blood cell anion transport protein. *Annu. Rev. Biophys. Biophys. Chem.* 18: 397–430, 1989.
16. JENNINGS, M. L., M. ADAMS-LACKEY, AND G. H. DENNEY. Peptides of human erythrocyte Band 3 protein produced by extracellular papain cleavage. *J. Biol. Chem.* 259: 4652–4660, 1984.
17. JENNINGS, M. L., M. P. ANDERSON, AND R. MONAGHAN. Monoclonal antibodies against human erythrocyte Band 3 protein. Localization of proteolytic cleavage sites and stilbenedisulfonate-binding lysine residues. *J. Biol. Chem.* 261: 9002–9010, 1986.
18. KHODADAD, J. K., AND R. S. WEINSTEIN. The Band 3-rich membrane of llama erythrocytes: studies on cell shape and the organization of membrane proteins. *J. Membr. Biol.* 72: 161–171, 1983.
19. KNAUF, P. A. Erythrocyte anion exchange and the Band 3 protein: transport kinetics and molecular structure. In: *Current Topics in Membranes and Transport*, edited by F. Bronner and A. Kleinzeller. New York: Academic, 1979, vol. 12, p. 249–363.
20. KNAUF, P. A., F.-Y. LAW, T. TARSHIS, AND W. FURUYA. Effects of the transport site conformation on the binding of external NAP-taurine to the human erythrocyte anion exchange system. Evidence for intrinsic asymmetry. *J. Gen. Physiol.* 83: 683–701, 1984.
21. LAEMMLI, U. K. Cleavage of structural proteins during the assembly of the head of bacteriophage T4. *Nature Lond.* 227: 680–685, 1970.
22. LAMBERT, A., AND A. G. LOWE. Chloride/bicarbonate exchange in human erythrocytes. *J. Physiol. Lond.* 275: 51–63, 1978.
23. MICHEL, F., AND V. RUDLOFF. Isolation and characterization of the rainbow trout erythrocyte band-3 protein. *Eur. J. Biochem.* 181: 181–187, 1989.
24. OHNISHI, S. T., AND H. ASAI. Lamprey erythrocytes lack glycoproteins and anion transport. *Comp. Biochem. Physiol. B Comp. Biochem.* 81: 405–407, 1985.
25. ROMANO, L., AND H. PASSOW. Characterization of anion transport system in trout red blood cell. *Am. J. Physiol.* 246 (*Cell Physiol.* 15): C330–C338, 1984.
26. STABENAU, E. K., T. A. HEMING, AND J. F. MITCHELL. Respiratory, acid-base, and ionic status of Kemp's ridley sea turtles (*Lepidochelys kempi*) subjected to trawling. *Comp. Biochem. Physiol. A Comp. Physiol.* 99: 107–111, 1991.
27. TOWBIN, H., T. STAEHELIN, AND J. GORDON. Electrophoretic transfer of proteins from polyacrylamide gels to nitrocellulose sheets: procedure and some applications. *Proc. Natl. Acad. Sci. USA* 76: 4350–4354, 1979.
28. WEBB, J. L. *Enzyme and Metabolic Inhibitors.* New York: Academic, 1963.
29. WESTERMAN, M. P., L. E. PIERCE, AND W. N. JENSEN. A direct method for the quantitative measurement of red cell dimensions. *J. Lab. Clin. Med.* 57: 818–824, 1961.
30. WHITE, F. N., AND P. E. BICKLER. Cardiopulmonary gas exchange in the turtle: a model analysis. *Am. Zool.* 27: 31–40, 1987.
31. WIETH, J. O. Bicarbonate exchange through the human red cell membrane determined with [^{14}C]bicarbonate. *J. Physiol. Lond.* 294: 521–539, 1979.
32. WIETH, J. O., O. S. ANDERSEN, J. BRAHM, P. J. BJERRUM, AND C. L. BORDERS, JR. Chloride-bicarbonate exchange in red blood cells: physiology of transport and chemical modification of binding sites. *Phil. Trans. R. Soc. Lond. B Biol. Sci.* 299: 383–399, 1982.
33. WIETH, J. O., AND J. BRAHM. Cellular anion transport. In: *The Kidney: Physiology and Pathophysiology*, edited by D. W. Seldin and G. Giebisch. New York: Raven, 1985, p. 49–89.
34. YAMAGUCHI, Y., K. D. JÜRGENS, H. BARTELS, P. SCHEID, AND J. PIIPER. Dependence of O_2 transfer conductance of red blood cells on cellular dimensions. *Adv. Exp. Med. Biol.* 222: 571–578, 1988.